Bottom-up Synthesis of Porous NiMo Alloy for Hydrogen Evolution Reaction

Kailong Hu, Samuel Jeong, Mitsuru Wakisaka, Jun-ichi Fujita and Yoshikazu Ito

Experimental methods

1. Calculation of turnover frequency (TOF).

The TOF values are calculated depend on the equation shown below [S1,S2].

$$\text{TOF } per \text{ site} = \frac{\#\text{Total Hydrogen Turn Overs / geometric area (cm}^2\text{)}}{\#\text{Surface Sites (Catalyst) /geometric area (cm}^2\text{)}}$$

The total number of hydrogen turn overs is calculated from the current density according to the following equation.

$$\#\text{H}_2 = \left(j\frac{\text{mA}}{\text{cm}^2}\right)\left(\frac{1\text{A}}{1000\text{ mA}}\right)\left(\frac{1\text{C}\cdot\text{s}^{-1}}{1\text{A}}\right)\left(\frac{1\text{mol } e^-}{96485.3\text{C}}\right)\left(\frac{1\text{mol H}_2}{2\text{ mol } e^-}\right)\left(\frac{6.02214\times10^{23}\text{ molecules H}_2}{1\text{ mol H}_2}\right)$$

$$= 3.12\times10^{15}\frac{\text{H}_2\text{ s}^{-1}}{\text{cm}^2}\,per\,\frac{\text{mA}}{\text{cm}^2}$$

The surface sites of catalyst are calculated as following:

$$\frac{\#\text{Surface Sites (Catalyst)}}{\text{geometric area (cm}^2\text{)}} = \frac{\#\text{Surface Sites (Flat Standard)}}{\text{geometric area (cm}^2\text{)}} \times \text{Roughness Factor}$$

The property of surface active sites of catalysts is still not well understood, and the accurate number of HER active sites for H desorption is also unknown. Therefore, we assume that the total surface sites as the active sites, including both Ni and Mo atoms. Due to the predominant presence of NiMo alloy on the surface, NiMo is taken as an example to show the calculation of active sites per surface area as below,

$$\frac{\#\text{Surface Sites (Flat Standard)}}{\text{geometric area (cm}^2\text{)}} = \left(\frac{56\text{ atoms } per \text{ unit cell}}{(734.32\times\text{Å})^3\ per \text{ unit cell}}\right)^{\frac{2}{3}} = 1.8\times10^{15}\text{ atoms/cm}^2\text{ surface area}$$

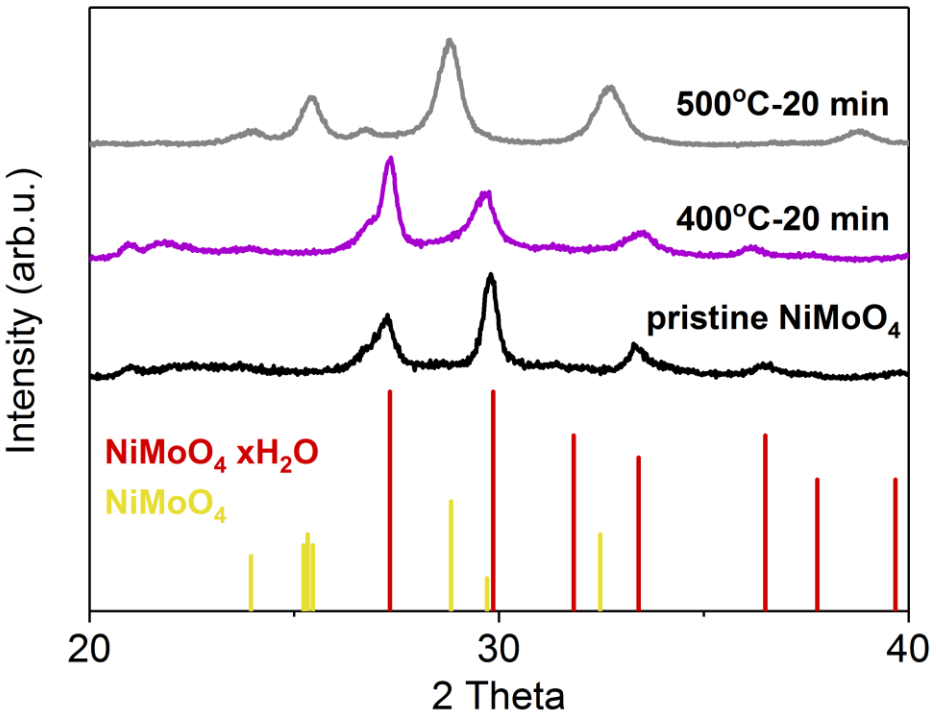

Figure S1. The XRD patterns of pristine $NiMoO_4$ and samples annealed at 400 and 500 °C for 20 min. The pristine $NiMoO_4$ and sample annealed at 400 °C match well with standard peaks of $NiMoO_4 \cdot xH_2O$ (JCPDS #13-0128). When the annealing temperature reached 500 °C, the crystalline water has been totally removed, and the peaks match well with $NiMoO_4$ (JCPDS #33-0948).

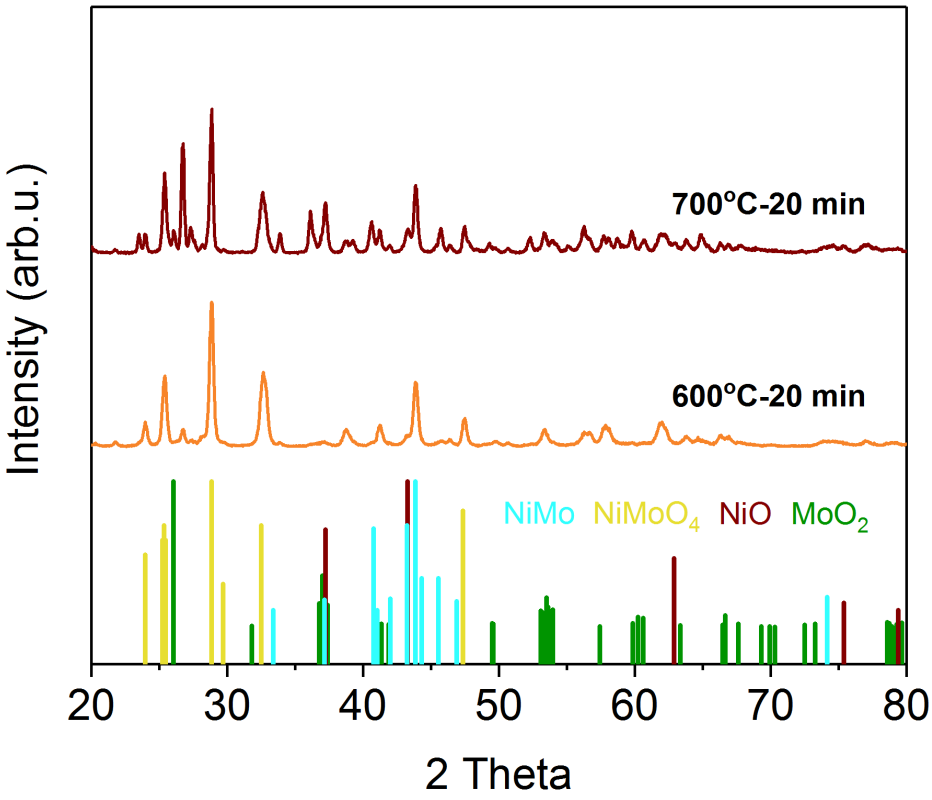

Figure S2. The XRD patterns of samples annealed at 600 and 700 °C for 20 min.

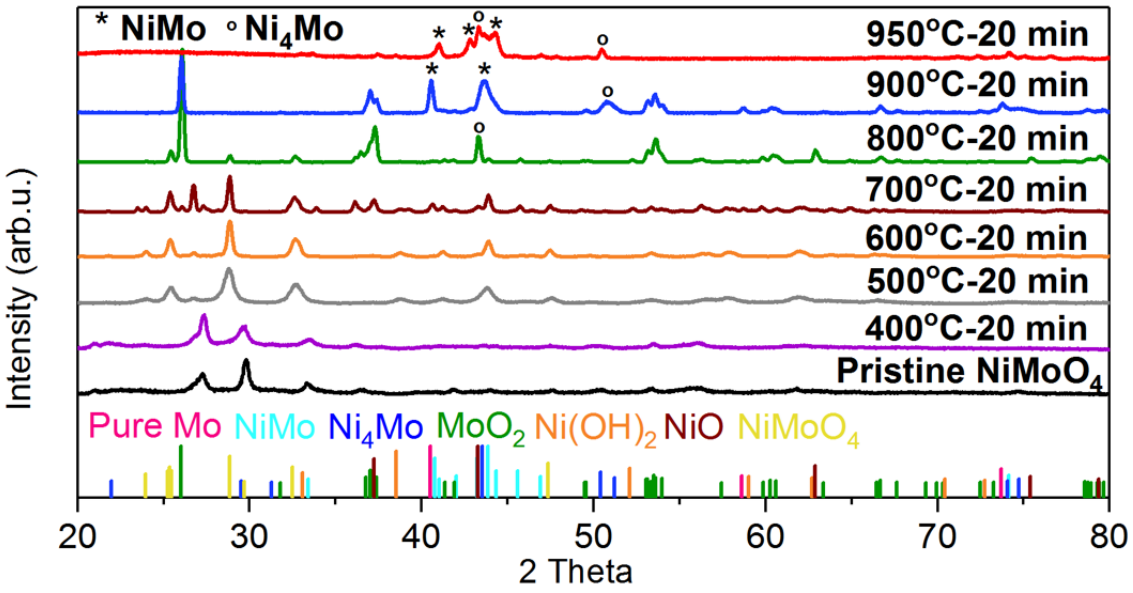

Figure S3. The overview of XRD patterns of pristine $NiMoO_4$ and samples annealed at temperature ranging from 400 to 950 °C for 20 min.

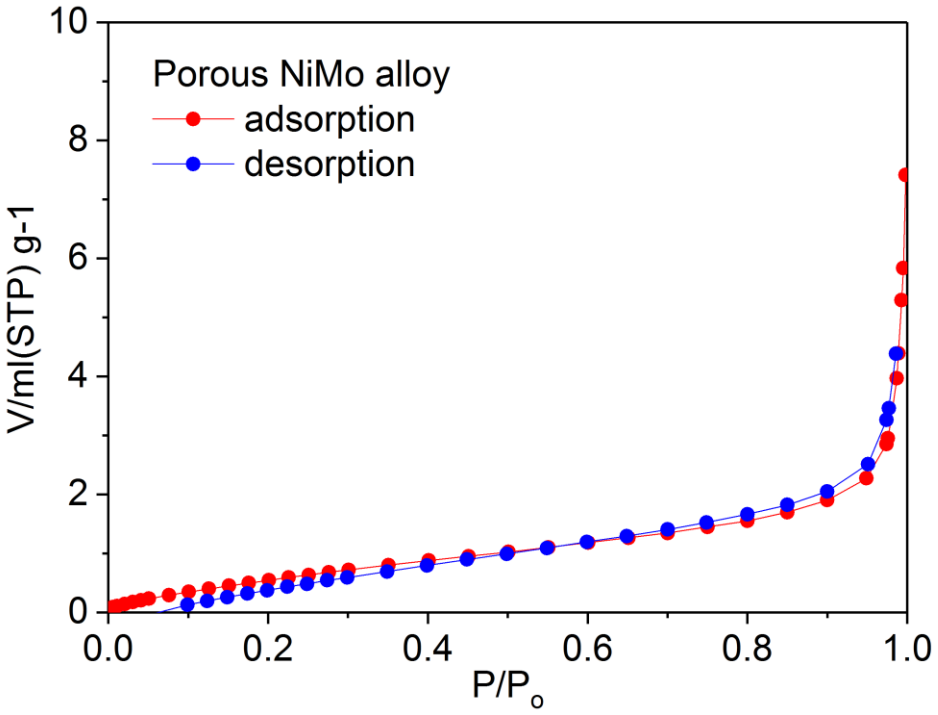

Figure S4. Nitrogen absorption and desorption measurements of porous NiMo alloy annealed at 950 °C for 20 min.

Table S1. The HER performances of porous NiMo alloy and other reported catalysts.

Catalyst	Onset Overpotential (mV)	Overpotential at 10 ($mA \cdot cm^{-2}$)	Tafel Slope (mV/decade)	TOF (s^{-1})	Electrolyte	Reference
3D porous NiMo	2	18	36	0.89 at −100 mV	1 M KOH	This work
NiMoN	32	109	95	-	1 M KOH	S3
CoP	-	54	51	-	1 M KOH	S4
$NiMoN_x/C$	78	300	36	-	0.1 M $HClO_4$	S5
NiCoP	-	167	71	0.056 at −100 mV	1 M KOH	S6
Mo_2C	37	112	55	-	0.1 M KOH	S7
NiMo nanopowders	20	126	-	-	1 M KOH	S8
WC/CNTs	45	150	106	-	0.1 M KOH	S9
$CoSe_2$	80	200	85	-	1 M KOH	S10
ZnCoS	40	100	48	-	0.1 M KOH	S11
Co/Co_3O_4	30	95	44	-	1 M KOH	S12
CoMoP@C	-	81	55	-	1 M KOH	S13
Ni_3S_2@NPC	30	61	68	-	1 M KOH	S14
Ni_4Mo	0	15	30	0.4 at −50 mV	1 M KOH	S15
NiCN	10	31	40	8.52 at −200 mV	1 M KOH	S16
$Ru@C_2N$	9.5	22	30	-	1 M KOH	S17
Ni_5P_4	-	49	98	0.79 at −100 mV	1 M KOH	S18

References

[S1] Benck, J.D.; Chen, Z.B.; Kuritzky, L.Y.; Forman, A.J.; Jaramillo, T.F. Amorphous molybdenum sulfide catalysts for electrochemical hydrogen production: Insights into the origin of their catalytic activity. *ACS Catal.* **2012**, *2*, 1916–1923.

[S2] Kibsgaard, J.; Tsai, C.; Chan, K.; Benck, J.D.; Nørskov, J.K.; Abild-Pedersen, F.; Jaramillo, T.F. Designing an improved transition metal phosphide catalyst for hydrogen evolution using experimental and theoretical trends. *Energy Environ. Sci.*, **2015**, *8*, 3022–3029.

[S3] Zhang, Y.Q.; Ouyang, B.; Xu, J.; Chen, S.; Rawat, R.S.; Fan, H.J. 3D porous hierarchical nickel–molybdenum nitrides synthesized by rf plasma as highly active and stable hydrogen-evolution-reaction electrocatalysts. *Adv. Energy Mater.* **2016**, *6*, 1600221.

[S4] Zhu, Y.P.; Liu, Y.P.; Ren, T.Z.; Yuan, Z.Y. Self-supported cobalt phosphide mesoporous nanorod arrays: A flexible and bifunctional electrode for highly active electrocatalytic water reduction and oxidation. *Adv. Funct. Mater.* **2015**, *25*, 7337.

[S5] Chen, W.F.; Sasaki, K.; Ma, C.; Frenkel, A.I.; Marinkovic, N.; Muckerman, J.T.; Zhu, Y.; Adzic, R.R. Hydrogen-evolution catalysts based on non-noble metal nickel-molybdenum nitride nanosheets. *Angew. Chem. Int. Ed.* **2012**, *51*, 6131.

[S6] Feng, Y.; Yu, X.-Y.; Paik, U. Nickel cobalt phosphides quasi-hollow nanocubes as an efficient electrocatalyst for hydrogen evolution in alkaline solution. *Chem. Commun.* **2016**, *52*, 1633.

[S7] Ma, F.X.; Wu, H.B.; Xia, B.Y.; Xu, C.Y.; Lou, X.W. Hierarchical β-Mo_2C nanotubes organized by ultrathin nanosheets as a highly efficient electrocatalyst for hydrogen production. *Angew. Chem. Int. Ed.* **2015**, *54*, 15395–15399.

[S8] McKone, J.R.; Sadtler, B.F.; Werlang, C.A.; Lewis, N.S.; Gray, H.B. Ni-Mo nanopowders for efficient electrochemical hydrogen evolution. *ACS Catal.* **2013**, *3*, 166–169.

[S9] Fan, X.; Zhou, H.; Guo, X. WC nanocrystals grown on vertically aligned carbon nanotubes: An efficient and stable electrocatalyst for hydrogen evolution reaction. *ACS Nano* **2015**, *9*, 5125–5134.

[S10] Chen, P.Z.; Xu, K.; Tao, S.; Zhou, T.P.; Tong, Y.; Ding, H.; Zhang, L.D.; Chu, W.S.; Wu, C.Z.; Xie, Y. Phase-transformation engineering in cobalt diselenide realizing enhanced catalytic activity for hydrogen evolution in an alkaline medium. *Adv. Mater.* **2016**, *28*, 7527–7532.

[S11] Huang, Z.-F.; Song, J.J.; Li, K.; Tahir, M.; Wang, Y.-T.; Pan, L.; Wang, L.; Zhang, X.W.; Zou, J.-J. Hollow cobalt-based bimetallic sulfide polyhedra for efficient all-pH-value electrochemical and photocatalytic hydrogen evolution. *J. Am. Chem. Soc.* **2016**, *138*, 1359–1365.

[S12] Yan, X.; Tian, L.; He, M.; Chen, X. Three-dimensional crystalline/amorphous Co/Co_3O_4 core/shell nanosheets as efficient electrocatalysts for the hydrogen evolution reaction. *Nano Lett.* **2015**, *15*, 6015–6021.

[S13] Ma, Y.-Y.; Wu, C.-X.; Feng, X.-J.; Tan, H.-Q.; Yan, L.-K.; Liu, Y.; Kang, Z.-H.; Wang, E.-B.; Li, Y.-G. Highly efficient hydrogen evolution from seawater by a low-cost and stable CoMoP@C electrocatalyst superior to Pt/C. *Energy Environ. Sci.* **2017**, *10*, 788–798.

[S14] Yang, C.; Gao, M.Y.; Zhang, Q.B.; Zeng, J.R.; Lia, X.T.; Abbott, A.P. In-situ activation of self-supported 3D hierarchically porous Ni_3S_2 films grown on nanoporous copper as excellent pH-universal electrocatalysts for hydrogen evolution reaction. *Nano Energy*, **2017**, *36*, 85–94.

[S15] Zhang, J.; Wang, T.; Liu, P.; Liao, Z.Q.; Liu, S.H.; Zhuang, X.D.; Chen, M.W.; Zschech, E.;

Feng, X.L. Efficient hydrogen production on $MoNi_4$ electrocatalysts with fast water dissociation kinetics. *Nat. Commun.* **2017**, *8*, 15437.
[S16] Yin, J.; Fan, Q.H.; Li, Y.X.; Cheng, F.Y.; Zhou, P.P.; Xi, P.X.; Sun, S.H. Ni–C–N nanosheets as catalyst for hydrogen evolution reaction. *J. Am. Chem. Soc.* **2016**, *138*, 14546–14549.
[S17] Mahmood, J.; Li, F.; Jung, S.-M.; Okyay, M.S.; Ahmad, I.; Kim, S.-J.; Park, N.; Jeong, H.Y.; Baek, J.-B. An efficient and pH-universal ruthenium-based catalyst for the hydrogen evolution reaction. *Nat. Nanotechnol.* **2017**, *12*, 441–447.
[S18] Laursen, A.B.; Patraju, K.R.; Whitaker, M.J.; Retuerto, M.; Sarkar, T.; Yao, N.; Ramanujachary, K.V.; Greenblatt, M.; Dismukes, G.C. Nanocrystalline Ni_5P_4: A hydrogen evolution electrocatalyst of exceptional efficiency in both alkaline and acidic media. *Energy Environ. Sci.* **2015**, *8*, 1027–1034.